Article

Not peer-reviewed version

Sentinel-2 Forel–Ule Index as a Proxy for Ecological Status in Reservoirs: A Case Study in Southern Portugal

Mariana Campista Chagas , Ana Paula Falcão , Rodrigo Proença de Oliveira *

Posted Date: 5 March 2026

doi: 10.20944/preprints202603.0477.v1

Keywords: Forel-Ule index; water quality; Water Framework Directive; Sentinel-2; Google Earth engine; ecological status of reservoirs

doi:10.20944/preprints202603.0477.v1

Article

Sentinel-2 Forel–Ule Index as a Proxy for Ecological Status in Reservoirs: A Case Study in Southern Portugal

Mariana Campista Chagas, Ana Paula Falcão and Rodrigo Proença de Oliveira *

Civil Engineering Research and Innovation for Sustainability (CERIS), Instituto Superior Técnico, Universidade de Lisboa, Av. Rovisco Pais 1, 1049-001 Lisboa, Portugal

* Correspondence: rodrigopoliveira@tecnico.ulisboa.pt

Highlights

- Sentinel-2–derived Forel–Ule Index (FUI) used to monitor 17 Mediterranean reservoirs in southern Portugal.
- FUI shows marked seasonal contrasts, distinguishing clearer and persistently colored, eutrophic reservoirs.
- PCA reveals a turbidity-driven trophic gradient moderately correlated with FUI.
- Ordinal logistic regression links FUI to Water Framework Directive ecological classes, with good skill for "Good" status at low FUI.
- FUI demonstrated as a low-cost, high-frequency screening and early-warning tool, complementary to conventional WFD monitoring.

Abstract

Water colour is an important optical proxy for trophic status and water quality, but its integration into regulatory assessment frameworks is still limited. This study assesses the potential of the Forel–Ule Index (FUI) derived from Sentinel-2 as a proxy indicator to support the assessment of the ecological status of reservoirs under the European Union's Water Framework Directive (WFD). Seventeen reservoirs located in semi-arid Mediterranean climate agricultural basins in southern Portugal (Sorraia, Sado, and Guadiana) were analysed, combining 4,316 FUI observations (2017–2024) with *in situ* water quality data and official WGD ecological status classifications. FUI values covered virtually the entire scale (1–21), with most observations between 12 and 18 and with marked spatial and seasonal contrasts, particularly between more transparent reservoirs and persistently turbid ones, probably eutrophicated reservoirs. Principal component analysis showed that the first component (PC1, 39.5% of variance) represents a trophic gradient dominated by turbidity, chemical oxygen demand and chlorophyll-a, and is positively, albeit moderately, correlated with FUI (Spearman's $\varrho = 0.439$, $p < 0.001$), while the second component, dominated by nitrogen, showed no significant association. The ordinal logistic regression relating the FUI to the ecological status classes of the WFD captured the expected quality gradient, with FUI values between 10–13 reliably identifying the status 'Good' (probability > 0.70), but with greater uncertainty for the intermediate range (14–16) and a tendency to underestimate "Poor/Bad" conditions when the FUI > 16. Overall, the FUI proves to be a low-cost, high-frequency screening and early warning tool that is effective in detecting good conditions and state transitions. However, it should be complemented by physical-chemical and biological metrics when a fine distinction between WFD classes is required.

Keywords: Forel-Ule index; water quality; Water Framework Directive; Sentinel-2; Google Earth engine; ecological status of reservoirs

1. Introduction

Monitoring water quality in reservoirs is essential to ensure water security and to protect ecological balance, constituting a central component of river basin management. However, the financial and logistical costs associated with conventional monitoring programs are often substantial, which justifies the exploration of alternative approaches based on proxy indicators. Water color is a particularly suitable indicator for assessing water quality and trophic status, as it is directly influenced by optically active constituents such as suspended sediments, dissolved organic matter, chlorophyll-a, and phytoplankton (Song et al., 2023). Variations in water color can reflect changes driven by natural processes, seasonal dynamics, climatic events, and anthropogenic activities (Lehmann et al., 2018).

The Water Framework Directive (Directive 2000/60/EC), adopted in 2000, constitutes the European Union's principal legal framework for the sustainable management and protection of water resources. Its overarching objective is to ensure that all water bodies, including reservoirs, achieve at least "good status," while preventing further deterioration and promoting the restoration of aquatic ecosystems. For reservoirs, ecological status assessment is a central component of the Directive and reflects the structural and functional integrity of the aquatic ecosystem in comparison with type-specific reference conditions minimally affected by anthropogenic pressures. Ecological status is determined through the evaluation of four main groups of elements: biological, physico-chemical, hydromorphological, and specific pollutants. Biological quality elements in reservoirs primarily include phytoplankton and fish (ichthyofauna), which are assessed using standardized indices and classified into five status classes (high, good, moderate, poor, and bad). Supporting physico-chemical elements comprise parameters such as dissolved oxygen, nutrient concentrations, and other regulated substances, evaluated against established thresholds and statistical criteria. Hydromorphological elements address the physical structure and hydrological regime of the reservoir, including aspects such as water level fluctuations and connectivity. In accordance with the "one-out, all-out" principle established by the Directive, the overall ecological status of a reservoir is determined by the lowest classification assigned to any of the assessed elements.

Directive 2000/60/EC established an initial period of fifteen years from its entry into force for achieving the established environmental objectives. However, it provides for the possibility of extensions for up to two additional six-year cycles—potentially extending the deadline until 2027—provided such extension is duly justified by technical, financial, or natural constraints, and that no further deterioration in the condition of the water bodies occurs during this period.

Assessing ecological status requires consistent and regularly collected data. However, traditional monitoring methods are often constrained by high costs, complex logistics, and low sampling frequency. Moreover, because assessments are typically conducted in pluri-annual cycles, the long intervals between surveys may hinder the adequate detection of significant events and rapid environmental changes. Regulatory agencies also frequently face limitations in the availability of continuous data, leading to temporal gaps that compromise a timely understanding of ecological dynamics. Collectively, these constraints hinder the effective implementation of preventive, corrective, and regulatory measures (Santos et al., 2018; APA, 2022).

In this scenario, tools such as the Forel-Ule Index (FUI) can play an important role in overcoming the limitations of traditional monitoring methods. This index classifies water color in bodies of water, ranging from deep blue to shades of green, brown, and yellow, according to their physical and chemical composition. Quantified on a scale of 1 to 21, it corresponds to the perceived color of the water (Lai et al., 2024; Xia et al., 2024). Its variations signal processes such as eutrophication, algal blooms, or changes in turbidity (Zhou et al., 2021; Song et al., 2023).

The FUI is largely calculated from satellite imagery, including MODIS, Landsat, and Sentinel II. By providing a low-cost solution and reduced reliance on field campaigns (Chen et al., 2021), it overcomes key limitations of conventional monitoring approaches while ensuring broad geographic coverage, objectivity and standardization (Ying et al., 2024; Li et al., 2024). Recent studies demonstrate its application across different spatial scales and water body types (Chen et al., 2021; Li et al., 2024;

Zhou et al., 2021a). For example, Chen et al. (2021) used MODIS data to analyse spatiotemporal variations in water colour in Chinese lakes, correlating changes in FUI with climatic and anthropogenic influences. Similarly, Xia et al. (2024) developed a method for FUI inversion in large reservoirs using the same sensor. However, both studies highlight the limitation of MODIS' low spatial resolution for smaller reservoirs. Zhou et al. (2021a) improved methods for obtaining the Forel-Ule index with Landsat 8 and Sentinel satellite images, highlighting the importance of atmospheric correction. This study demonstrated that methodological improvements increase the accuracy and reliability of estimates derived from remote sensing. Li et al. (2024), using Sentinel-2 images, identified seasonal patterns of FUI variation in 523 Chinese urban lakes, revealing a predominance of green tones (>80%) and spatial heterogeneity: lakes in arid and northern regions had higher FUI than those in humid and southern areas. Panoramic urban lakes exhibited lower indices than non-panoramic lakes, suggesting a positive influence of management practices (water replenishment, cleaning).

FUI can be related to parameters such as chlorophyll-a, phosphorus, and nitrogen, which are essential for assessing trophic state and monitoring cyanobacterial blooms (Chen et al., 2021; Zhou et al., 2021a; Song et al., 2023). Studies such as Lai et al. (2024) highlight the sensitivity of FUI in capturing important local variations in trophic state and turbidity in large reservoirs. Zhao et al. (2023) demonstrated that the integration of Sentinel-2 satellite data, FUI, and Gaussian Process Regression (GPR) improves trophic state monitoring in urban aquatic environments. These authors also highlight the influence of anthropogenic and meteorological factors, such as temperature and wind speed, on eutrophication, reinforcing the need for continuous validation of these approaches. To automate monitoring, Song et al. (2023) presented advances using Google Earth Engine (GEE) to map cyanobacterial blooms, employing the FUI to identify changes in water color associated with these events.

Despite methodological and technological advances, a gap remains in the implementation of continuous and high-frequency monitoring systems, particularly in inland waters located in arid or difficult-to-access regions. This study uses the FUI as a proxy indicator to identify water bodies that require further investigation, directing resources to reservoirs with signs of environmental concerns or deviations from expected ecological conditions. The application of the FUI can contribute to overcoming current constraints, enabling more frequent and spatially comprehensive assessments, better aligned with regulatory demands.

In this context, the objectives of this study are:

(1) To calculate the Forel–Ule Index (FUI) from Sentinel-2 images, using advanced processing and segmentation techniques in Google Earth Engine (GEE), and to characterize its seasonal variability across 17 reservoirs in southern Portugal.

(2) To investigate environmental gradients and multivariate patterns that relate the FUI to key physical-chemical parameters of water quality in reservoirs.

(3) To compare FUI-based patterns with the ecological status classifications established under the Water Framework Directive (Directive 2000/60/EC), evaluating the potential and limitations of the FUI as a proxy indicator for regulatory assessment purposes.

2. Materials and Methods

2.1. Image Selection and Calculation of FUI from Sentinel-2

This study used data from the Multispectral Instrument (MSI) sensors on board the Sentinel-2 satellite to calculate the Forel-Ule Index (FUI) in each reservoir analyzed. The data was acquired, pre-processed and processed on the Google Earth Engine (GEE) cloud platform, covering the period from October 2018 to September 2024. For each reservoir, images were selected from this time interval with up to 5% cloud cover. In addition, a specific mask was applied to remove clouds and cirrus clouds based on the QA60 quality band, using the cloudBitMask (bit 10) and cirrusBitMask (bit 11) masks to discard contaminated pixels.

 doi:10.20944/preprints202603.0477.v1

The number of images used per reservoir varied according to the spatial extent of each study area, with an average of 200 scenes per reservoir and a range between 136 and 387 images, totaling 4316 images for the entire analysis. Sentinel-2 bands B1, B2, B3, B4 and B5 were used to calculate the FUI. Bands B1 and B5, originally with spatial resolutions of 60 m and 20 m, respectively, were reprojected and resampled to a uniform resolution of 10 meters, using the projection of band B2 as a reference.

Linear expressions were applied to the bands B1, B2, B3, B4 and B5 , according to specific weights, resulting in the tristimulus values X, Y and Z, according to the following equations drawn up by (Wang et al., 2015; Gardner et al, 2021; Ye and Sun, 2022):

$$X = 8{,}356 \cdot \mathrm{B1} + 12{,}040 \cdot \mathrm{B2} + 53{,}696 \cdot \mathrm{B3} + 32{,}087 \cdot \mathrm{B4} + 0{,}487 \cdot \mathrm{B5}$$

$$Y = 0{,}993 \cdot \mathrm{B1} + 23{,}122 \cdot \mathrm{B2} + 65{,}702 \cdot \mathrm{B3} + 16{,}830 \cdot \mathrm{B4} + 0{,}177 \cdot \mathrm{B5}$$

$$Z = 43{,}487 \cdot \mathrm{B1} + 61{,}055 \cdot \mathrm{B2} + 1{,}778 \cdot \mathrm{B3} + 0{,}015 \cdot \mathrm{B4} \qquad (1)$$

where, B1 to B5 correspond to the Sentinel-2 spectral bands.

Chromatic coordinates were calculated by:

$$x = \frac{X}{(\mathrm{X+Y+Z})}; \mathrm{y} = \frac{\mathrm{Y}}{(\mathrm{X+Y+Z})} \qquad (2)$$

The normalized x and y coordinates were adjusted by subtracting 0.33 (center of chromatic space), resulting in x_adj and y_adj:

$$\mathrm{x_{adj}} = \mathrm{x} - 0{,}33;\ \mathrm{y_{adj}} = \mathrm{y} - 0{,}33 \qquad (3)$$

Based on the adjusted components, the spectral angle ($angle_{hue}$) was calculated, corrected for complete quadrants (0° to 360°), considering the signal ratios of x_adj and y_adj. The hue angle for each pixel is obtained by:

$$\mathrm{angle} = \arctan\left(\mathrm{x_{adj}} / \mathrm{y_{adj}}\right) + \begin{cases} 2\pi, \text{se } \mathrm{y_{adj}} > 0 \\ \pi, \text{se } \mathrm{y_{adj}} < 0 \end{cases} \qquad (4)$$

The angle was then converted to degrees for the adjustment:

$$angle_{degree} = (180 / \pi) * \mathrm{angle}$$

$$angle_{hue} = angle_{degree} - 360 \qquad (5)$$

The continuous value of was transformed into discrete Forel-Ule classes (FUI 1 to FUI 21) by means of empirically defined angular thresholds. The angle hue classification in the Forel-Ule Index (FUI) establishes the correspondence between angle hue ranges (in degrees) and the 21 FUI classes. It is based on increasing angle hue values, which represent gradual variations in water color tone: more negative angles (FUI classes 1 to 5) are associated with bluish hues; intermediate classes (FUI 6 to 16) encompass transitions from green to yellowish-green; and higher positive angles (FUI classes 20 and 21) correspond to brownish hues. These color variations reflect different optical compositions of the water column, with bluish hues indicating clearer water, while yellowish and brownish hues are often related to a greater presence of phytoplankton, dissolved organic matter, and suspended solids. This categorization, adapted from Wang et al. (2015), provides an objective framework for converting spectral data into FUI classes, allowing standardization and comparison between in situ measurements and observations derived from remote sensing.

The final FUI value calculated for each pixel was stored in the respective FUI band of each processed image. For each scene in the time series, descriptive statistics were extracted for the FUI variable within the spatial cut-off for each reservoir. The metrics calculated included minimum value (min), maximum value (max), mean, median, mode, 25th and 75th percentiles and standard deviation (stdDev). These statistics were consolidated into a Feature Collection, in which each feature represents a specific date in the time series. Finally, temporal analyses were carried out on this data, allowing a detailed assessment of the variations in FUI over the period studied in each reservoir.

 doi:10.20944/preprints202603.0477.v1

2.2. Investigation of Relationships with Water Quality Parameters

Five water quality parameters obtained from in situ measurements were considered: total phosphorus, total nitrogen, chlorophyll-a, chemical oxygen demand (COD), and turbidity. These data were retrieved from monitoring records of large public reservoirs available through the National Water Resources Information System (SNIRH). As SNIRH provides measurements only for specific sampling dates, the available dates for each parameter were identified separately for each reservoir. To enable comparison with the Forel–Ule Index (FUI) derived from remote sensing, Sentinel-2 observations acquired on the same date as the in situ measurements, or within a maximum temporal window of ±3 days, were selected from the processed image collection.

The data was structured in columns, including the date and the respective water quality parameters for all the reservoirs analyzed. It should be noted that the sampling dates for the different parameters coincided, ensuring temporal comparability between the variables considered.

To investigate the interrelationships between the Forel-Ule Index (IUF) and the physical-chemical parameters of water, Principal Component Analysis (PCA), a multivariate statistical tool (Hotelling, H., 1933), was used. Although the physical-chemical parameters analyzed (phosphorus, nitrogen, turbidity, chlorophyll-a, and chemical oxygen demand) do not show a significant correlation with the FUI in isolation, PCA was applied to reveal hidden structural patterns in the data. PCA allows the identification of latent environmental gradients resulting from interrelated combinations, which may not be detectable through traditional univariate analyses.

Consequently, even in the absence of individual linear correlations, the FUI can align with one or more principal components that synthesize the variability of water quality indicators. Additionally, PCA enables the identification of the main environmental gradients that underline this variability, especially in contexts where multiple indicators are obtained by different methods (Jolliffe & Cadima, 2016; Hair et al., 2019).

2.3. Analysis of the Relationship Between the Forel-Ule Index and the Ecological Status of Reservoirs

To evaluate the relationship between the Forel–Ule optical index (FUI) and the ecological status classification under the Water Framework Directive (WFD), official ecological status classifications for the second (2018–2021) and third (2022–2024) WFD management cycles were compiled from the Portuguese Environment Agency (APA) for the selected reservoirs. These datasets included both the overall ecological status classifications and the corresponding component assessments, namely biological, physico-chemical, hydromorphological elements, and specific pollutants (Table 1). In accordance with the Directive's "one-out, all-out" principle, the overall ecological status of a reservoir is determined by the lowest classification assigned to any of the assessed quality elements. As indicated in Table 1, the biological quality element most frequently determines the final ecological status classification.

Table 1. Ecological status and elements in accordance with the Water Framework Directive. Source: National Water Resources Information System (https://snirh.apambiente.pt/).

Cycle	Reservoir	Ecological status	Biological	Physico-chemical	Hydro morphological	Pollutants
Second Cicle	Alvito	Good	Good	Good	No data	No data
	Beliche	Good	Good	Good	No data	Good
	Caia	Moderate	No data	Moderate	No data	Good
	Campilhas	Good	Good	Good	No data	Good
	Divor	Moderate	Moderate	Moderate	No data	Good
	Magos	Moderate	Moderate	Moderate	No data	Good
	Maranhao	Moderate	Moderate	Moderate	No data	Good
	Minutos	Good	Good	Good	No data	Good

	Montargil	Moderate	Moderate	Moderate	No data	Good
	Monte da Rocha	Good	Good	Good	No data	Good
	Monte Novo	Moderate	Moderate	Moderate	No data	Good
	Odeleite	Good	Good	Good	No data	Good
	Odivelas	Good	Good	Good	No data	Good
	Pego do Altar	Good	Good	Good	No data	Good
	Roxo	Good	Good	Good	No data	Good
	Vale do Gaio	Moderate	Moderate	Moderate	No data	Good
	Vigia	Moderate	Moderate	Moderate	No data	Good
Third cicle	Alvito	Moderate	Moderate	Moderate	Moderate	Moderate
	Beliche	Good	Excellent	Excellent	Excellent	Good
	Caia	Moderate	Good	Moderate	Excellent	Good
	Campilhas	Moderate	Moderate	Good	Excellent	Good
	Divor	Bad	Bad	Moderate	Excellent	Good
	Magos	Poor	Poor	Moderate	Excellent	Good
	Maranhao	Poor	Poor	Moderate	Excellent	Moderate
	Minutos	Good	Good	Good	Excellent	Good
	Montargil	Moderate	Moderate	Good	Excellent	No data
	Monte da Rocha	Moderate	Moderate	Moderate	Excellent	Moderate
	Monte Novo	Moderate	Moderate	Moderate	Excellent	Moderate
	Odeleite	Good	Excellent	Excellent	Excellent	Good
	Odivelas	Moderate	Moderate	Good	Excellent	Good
	Pego do Altar	Moderate	Moderate	Moderate	Excellent	Good
	Roxo	Moderate	Moderate	Good	Good	Good
	Vale do Gaio	Moderate	Moderate	Moderate	Excellent	Good
	Vigia	Moderate	Moderate	Moderate	Good	Good

The compiled dataset comprised: (i) the overall ecological status classification for each cycle; (ii) the individual classifications of its components (biological, hydromorphological, physico-chemical, and specific pollutants; see Table 1); and (iii) the mean FUI values calculated for each reservoir over the corresponding cycle periods. To enable statistical modelling, ecological status classes were converted into an ordinal numerical scale reflecting the hierarchical structure defined by the WFD: High (0) < Good (1) < Moderate (2) < Poor (3) < Bad (4).

Ordinal logistic regression (LogisticAT model, mord package in Python) was applied to analyze the association between the Forel-Ule index and the APA parameters. Logistic regression was used to investigate the relationship between a categorical response variable (quality classes) and the explanatory variable (FUI). Unlike linear regression, which estimates continuous outcomes, logistic regression applies to the logit function (logarithm of the odds ratio) to express the probability of class membership as a linear function of the predictors (McCullagh, 1980).

Therefore, the probability of a given class was estimated as a function of the explanatory variable, making this approach suitable for analyzing and predicting categorical outcomes. This model was selected for its ability to handle ordinal variables, allowing the assessment of how the FUI influenced the probability of classification across ecological status classes. For each observation, the model provided the predicted class and the associated probability distribution, which enabled comparisons between observed values (official APA data) and estimated values, as well as an evaluation of the sensitivity of the Forel-Ule index in distinguishing among quality classes.

 doi:10.20944/preprints202603.0477.v1

3. Case Study

The study focuses on 17 reservoirs located in the Sorraia (7,730 km²), Guadiana (11,600 km² in Portugal) and Sado (7,700 km²) river basins, situated in a semi-arid Mediterranean climate (Csa) region of southern Portugal (Figure 1). This region is characterised by hot, dry summers and mild, wet winters, with most of the annual precipitation (600–800 mm) occurring between October and May, and mean annual air temperatures ranging from 16 to 19 °C.

From both hydrological and land-use perspectives, the study area represents one of the most water-stressed and anthropogenically pressured semi-arid regions in Portugal. Average annual precipitation (636 mm) is substantially lower than mean annual evapotranspiration (1,337 mm), resulting in a marked hydrological deficit (European Environment Agency, 1996). Intensive land use, agricultural expansion, deforestation, and urban development exert significant pressures on water quality by promoting the runoff of nutrients, pesticides, and other pollutants into aquatic systems. Consequently, reservoirs in this region are particularly vulnerable to eutrophication, cyanobacterial blooms, the accumulation of toxic compounds, and habitat degradation (Molina-Navarro et al., 2020; Rocha & Rocha, 2023; Sampath & Boski, 2016).

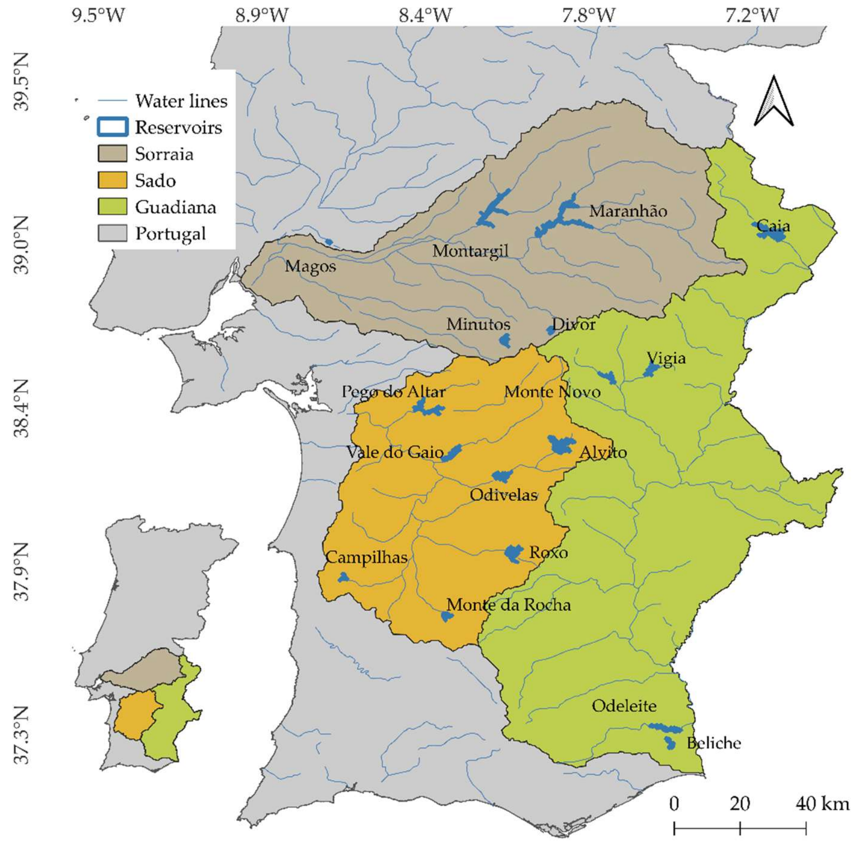

Figure 1. Study area. Location of reservoirs in the Sorraia, Sado, and Guadiana River basins.

The Sorraia River Basin is characterised by intensive agricultural use, with irrigated land covering approximately 16,000 ha, primarily dedicated to maize, rice, and tomato production. Irrigation water is regulated through the Montargil and Maranhão reservoir systems (Almeida et al., 2018). Although the basin includes residential and industrial areas, agriculture remains the dominant activity and constitutes the main driver of water quality pressures. In comparison, urban pollution sources are relatively limited. Of the 122 water bodies assessed in the basin (predominantly rivers), 24% are classified as having moderate or lower ecological status (Table 1). The primary cause of degradation is associated with intensive water abstraction for irrigation, which accounts for

 doi:10.20944/preprints202603.0477.v1

approximately 26% of the total water demand in the Tagus basin. Irrigation supports around 16,500 ha and consumes approximately 120 × 10^6 m^3 of water annually (Molina-Navarro et al., 2020).

The Sado River Basin is situated in one of the most arid regions of Portugal. Although industrial activities are concentrated around Setúbal, the Sado estuary, and the Port of Sines, agriculture remains the dominant land use. Agricultural water demand is largely supported by multiple reservoir systems, supplemented by inter-basin water transfers from the Guadiana basin (APA, 2022b). Water quality in the Sado basin is influenced by several interacting pressures, including intensive land use, deforestation, and agricultural practices that enhance surface runoff and soil erosion, thereby increasing the transport of sediments and pollutants into aquatic systems (Matono et al., 2013). The expanding use of agrochemicals, particularly pesticides, underscores the need for continuous monitoring to assess contamination risks (Rocha & Rocha, 2023). Furthermore, studies of water and sediment quality in the Sado estuary have documented the presence of endocrine-disrupting compounds, with potential impacts on aquatic biota and implications for water intended for human consumption (Rocha et al., 2013; Nascimento et al., 2021).

The Guadiana River Basin has undergone profound transformation since the early 2000s, particularly with the development of the Alqueva system, which significantly reshaped regional water management dynamics (APA, 2022a). With a storage capacity of 4,150 Mm^3, the Alqueva reservoir represents the largest strategic water reserve in Portugal. It underpins an extensive irrigation network connecting more than 70 secondary reservoirs and supplying water to approximately 150,000 ha of agricultural land, where olive groves, cereals, vineyards, nuts, and horticultural crops predominate (EDIA, 2022). Water quality in the Guadiana River and its estuary is strongly influenced by anthropogenic pressures, including intensive agriculture, urban expansion, and flow regulation by dams—particularly the Alqueva dam. Large-scale hydrological regulation has altered the river's natural flow regime and ecological balance, reducing seasonal flow variability and flood pulses. These changes have increased water residence times, promoted stagnation and contributing to water quality deterioration in certain stretches of the basin (Palma, 2009; Sampath & Boski, 2016).

Table 2 shows the main physical and operational characteristics of the reservoirs evaluated, along with the average values of the water quality parameters observed during the study period.

Table 2. Main characteristics of the reservoirs. Source: National Water Resources Information System (https://snirh.apambiente.pt/).

Reservoirs	Main Use	Net Capacity (dam3)	Dead Storage Volume (dam3)	Minimum Operating Level (m)	Inundation Area at Full Level (ha)
Alvito	Human supply	130000	2500	172	1480
Beliche	Human supply	47600	400	15	292
Caia	Irrigation	192300	10700	192.4	1970
Campilhas	Irrigation	26156	1000	92.53	333
Divor	Irrigation	11890	10	249.5	265
Magos	Irrigation	2852	180	10.4	124
Maranhão	Irrigation	180900	24500	85.47	1960
Minutos	Irrigation	47400	2100	245	530
Montargil	Irrigation	142700	21600	65.05	1495
Mte da Rocha	Human supply	97760	5000	113.25	1100
Monte Novo	Various	14780	500	183.5	277.4
Odeleite	Irrigation	117000	13000	22	720
Odivelas	Irrigation	70000	26000	91.3	973
Pego do Altar	Irrigation	93600	400	15	655
Roxo	Irrigation	89512	6800	122	1378
Vale do Gaio	Irrigation	63000	0	11	550
Vigia	Human supply	15579	1146	210	262

 doi:10.20944/preprints202603.0477.v1

4. Results

4.1. Spatial and Seasonal Variation of the Forel-Ule Index

FUI values exhibit substantial variability among reservoirs, ranging from 1 to 21, with a mean value of 15 and a standard deviation of 3. Most observations clustered between 12 and 18. The median was 16, while the 25% and 75% percentiles were 13 and 18, respectively (Table 3; Figure 2).

Table 3. Descriptive statistics for the Forel-Ule index, including number of samples, mean, standard deviation, minimum and maximum values, and quartiles.

Statistic	Value
Count	4316
Mean	15
Std	3
Min	1
25th percentile	13
Median	16
75th percentile	18
Max	21

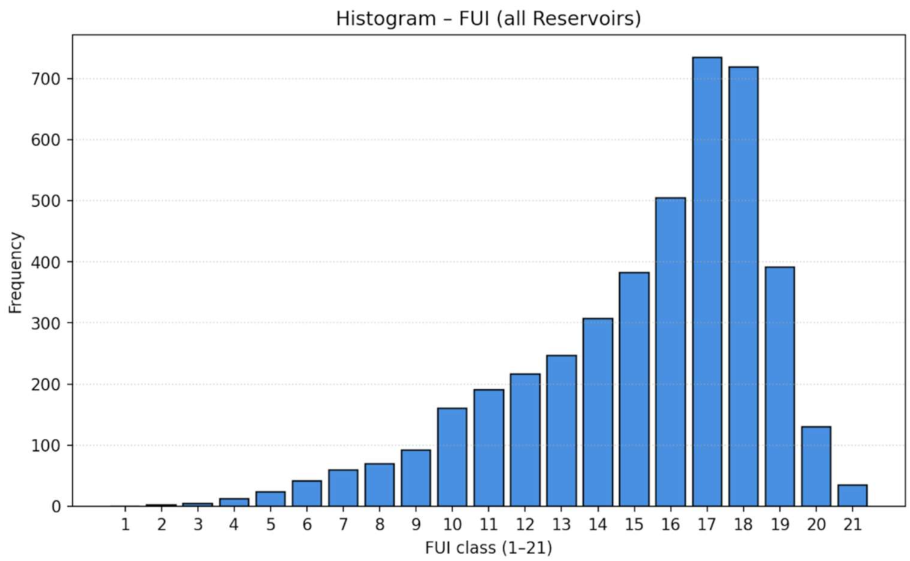

Figure 2. Frequency distribution of the FUI classes for all reservoirs combined. A higher concentration of observations is observed between classes 15 and 18, indicating the predominance of waters with intermediate to high coloration.

In addition to pronounced spatial differences among reservoirs, a marked seasonal variability was also observed (Figure 3).

Preprints.org (www.preprints.org) | NOT PEER-REVIEWED | Posted: 5 March 2026 doi:10.20944/preprints202603.0477.v1

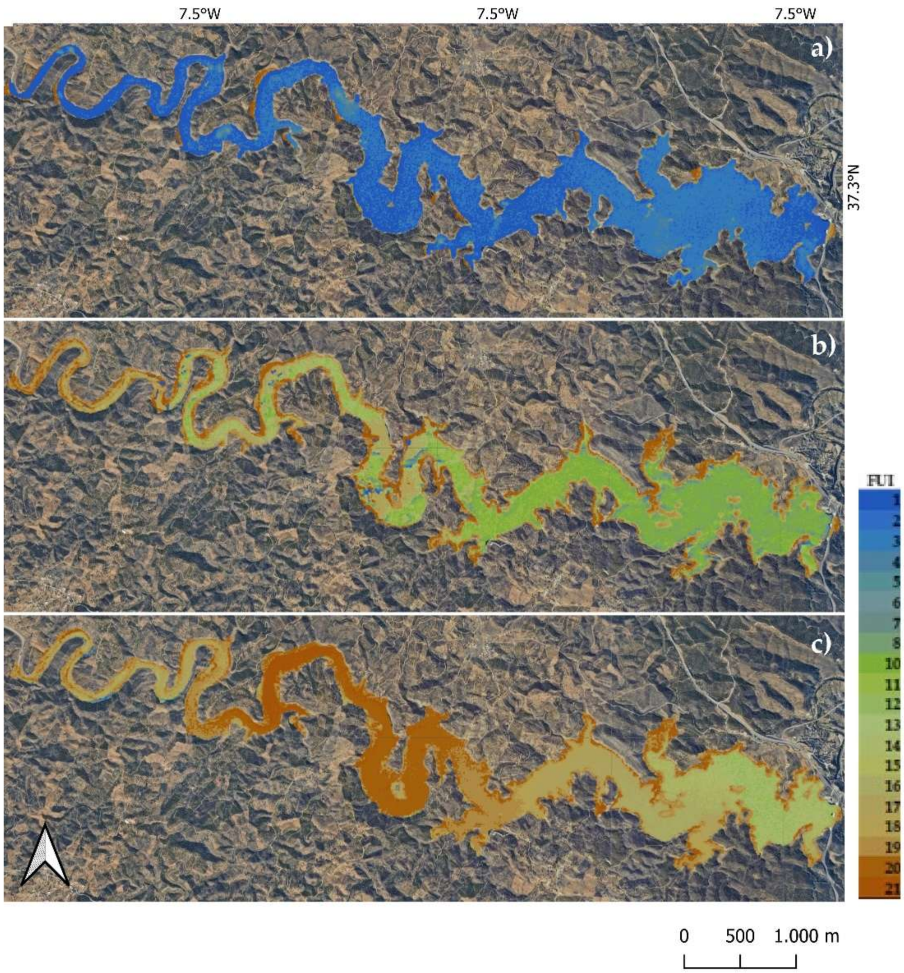

Figure 3. Variation of the Forel-Ule Index at different dates in the Odeleite reservoir: (a) June 2017, mean FUI of 4; (b) May 2020, mean FUI of 13; (c) January 2024, mean FUI of 18.4.1 Spatial and Seasonal Variation of the Forel-Ule Index in the Reservoirs.

Analysis of the Forel-Ule Index (FUI) heatmap over the years shows marked differences in the behavior of the various reservoirs (Figure 4). Some systems, such as Alvito, Beliche, Minutos, Odivelas, predominantly have the lowest FUI values, often below 14, reflecting more transparent waters and less eutrophied conditions. In these reservoirs, the FUI peaks are occasional, and the inter-annual variations are less marked, which may indicate less nutrient input, a better state of environmental conservation or less anthropogenic pressure.

In contrast, reservoirs such as Campilhas, Monte da Rocha, Vale do Gaio, Magos, Divor, Pego do Altar and Monte Novo show consistently high FUI values, especially during the spring and summer months, often exceeding 17. These patterns suggest a greater recurrence of coloured waters, potentially associated with eutrophication processes and the presence of high concentrations of organic matter and phytoplankton. In some of these reservoirs, high FUI values persist for long periods.

Reservoirs such as Caia, Maranhão, Montargil, Vigia and Roxo, on the other hand, show intermediate patterns, with FUI values that fluctuate more moderately over time and a predominance of intermediate values. Divor and Magos show a higher but relatively stable FUI trend over the years, while Caia, Alvito, Beliche and Odeleite show greater temporal variability in FUI values.

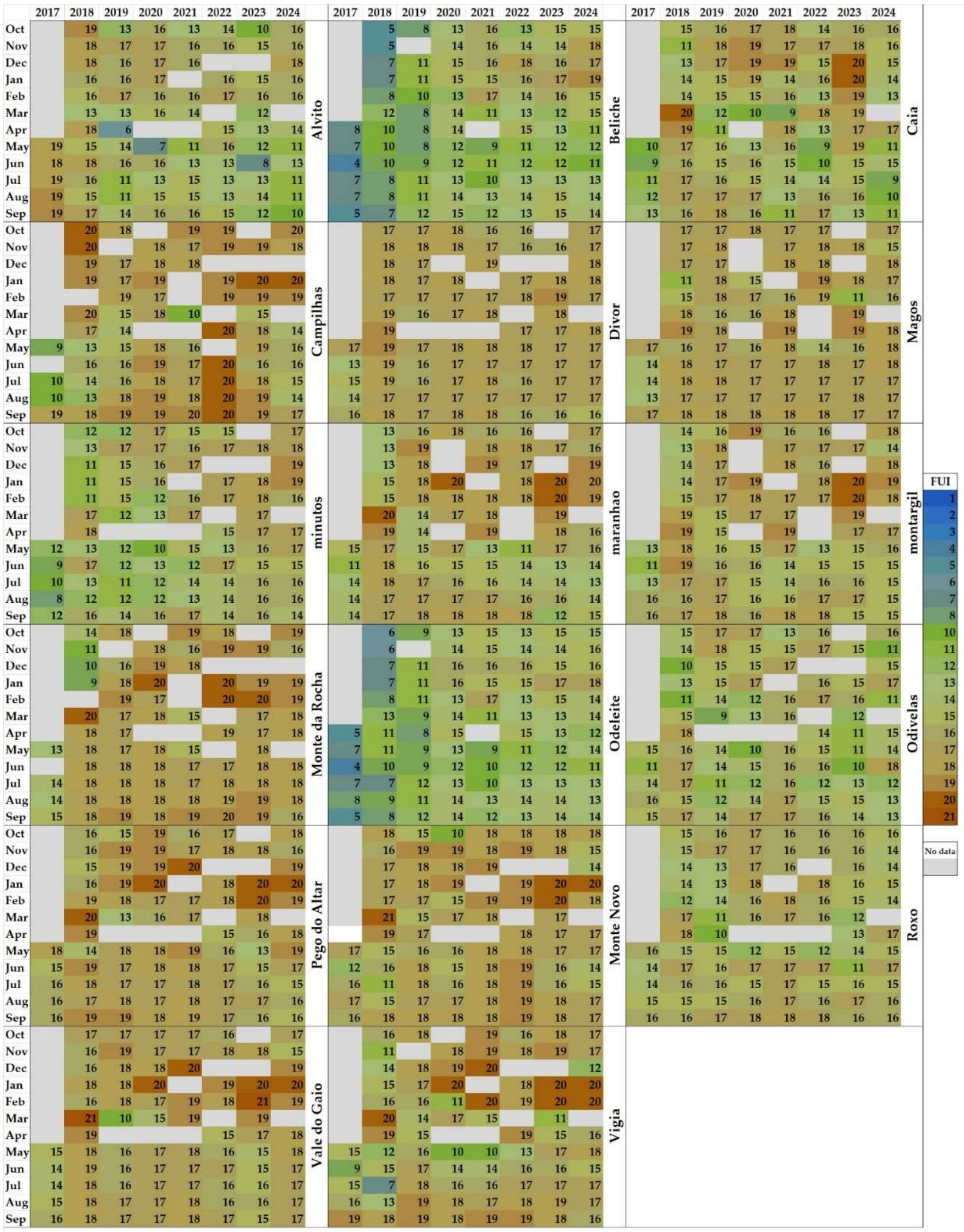

Figure 4. Heatmap of the Forel-Ule index (FU_mean) in the reservoirs, organized by month and year. Higher values of the index (in yellow) represent greater coloration of the water, while lower values (in purple/blue) indicate more transparent waters. Gray cells indicate no data for the corresponding period. The color bar on the right illustrates the variation in index values from 1 (minimum) to 21 (maximum).

Figure 5 illustrates the seasonal distribution of IUF values across the four seasons. The highest median values occur during fall and winter, while spring and summer have relatively lower medians. The interquartile ranges for fall and winter are narrower, indicating less dispersion of the central values in these seasons, with the data concentrated between the first and third quartiles. On the other hand, there is a wider interquartile range in spring and summer, suggesting greater data variability during these periods.

The presence of outliers also varies across seasons: fall has the highest number of extreme points below the first quartile, followed by winter and, to a lesser extent, summer. In spring, the incidence of outliers is less significant. Maximum values are similar across seasons, while the distribution of minimum values, represented primarily by outliers, is particularly notable in the months of March, May, and July.

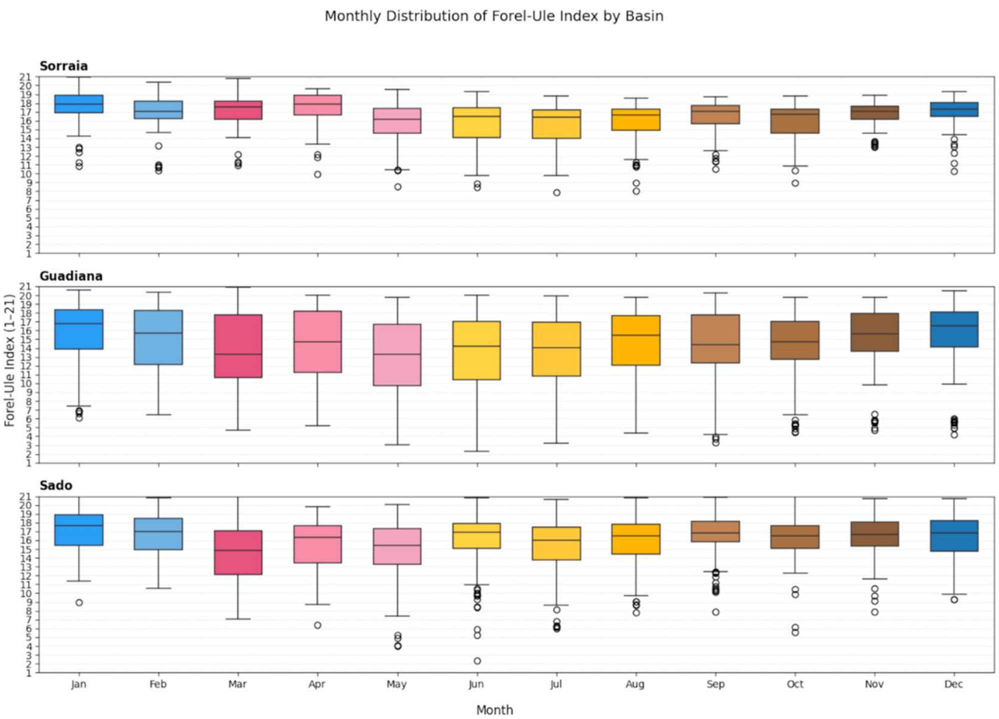

Figure 5. Monthly distribution of the Forel-Ule Index (FUI) for each watershed, across all reservoirs and over the years. Each box represents the variability of FUI values observed in each month from 2017 to 2024. The color scheme indicates the seasonal cycle: blue tones for winter (Dec–Feb), pink tones for spring (Mar–May), yellow tones for summer (Jun–Aug), and brown tones for autumn (Sep–Nov).

4.2. Multivariate Data Analysis

To prevent highly dispersed variables from exerting a disproportionate influence on the extraction of principal components, the sample outliers were removed. From the 423 initial samples, 24 were excluded because they were identified as outliers, resulting in a final set of 399 samples used in the multivariate analyses (Table 4).

Table 4. Initial and post-processing variance values for water quality parameters.

Parameter	Initial Variance	Post-Processing Variance
Phosphorus	0.0120	0.0015
Nitrogen	1.1061	0.7197
Chlorophyll	0.0026	0.0003
COD	73.3485	37.2460
Turbidity	145.669	22.0212

Figure 6 presents the variance of each environmental parameter before and after the elimination of outliers. This process resulted in a significant decrease of variance values, especially in what concerns turbidity (from 99.299 to 21.987) and chemical oxygen demand (COD) (from 45.088 to 36.965). Parameters such as phosphorus, nitrogen, and chlorophyll-a also showed a decrease in variance, albeit on a smaller scale.

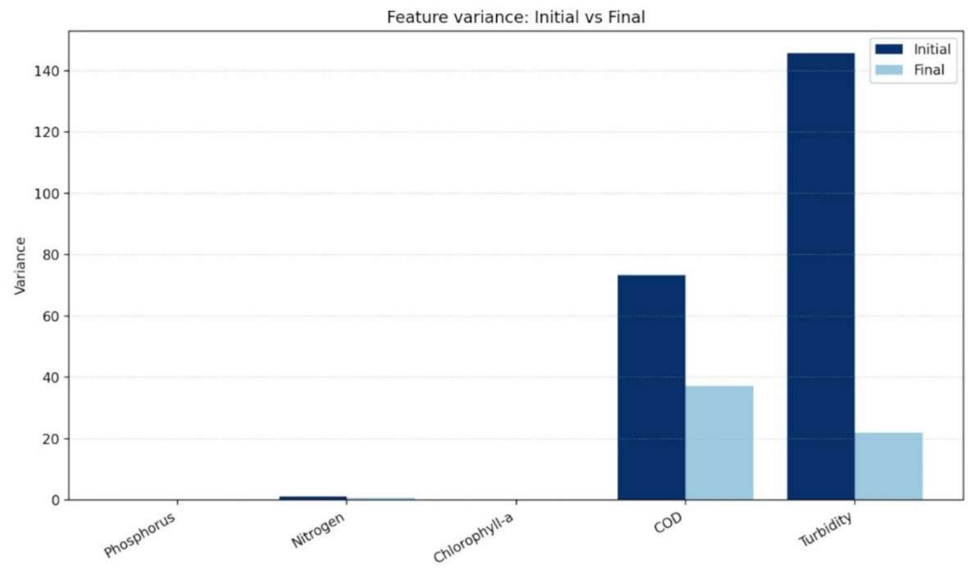

Figure 6. Initial variance and post-processing of water quality parameters, indicating reduced data dispersion after cleaning and standardization.

The PCA revealed that the first two components together explain approximately 62% of the total variance in the data (PC1: 39.5%; PC2: 22.9%) (Figure 7). The first principal component (PC1) is related to environmental parameters such as turbidity, chemical oxygen demand (COD), chlorophyll-a, and phosphorus, reflecting a trophic quality gradient of the water, while the second component is dominated by nitrogen and to a lesser extent phosphorus (Table 5).

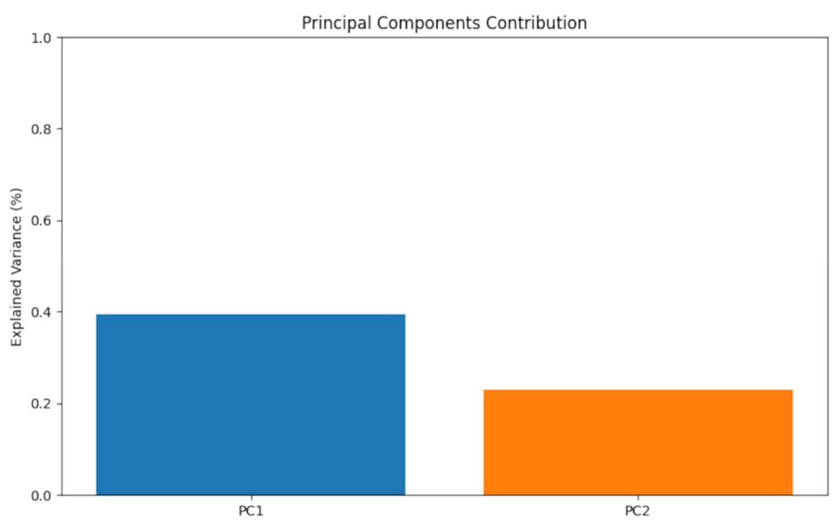

Figure 7. Proportion of total variance explained by PC1 (~39%) and PC2 (~23%), totaling approximately 62%.

The analysis of factor loadings in Table 5 revealed that the first principal component (PC1) is strongly influenced by turbidity (0.591), COD (0.493), chlorophyll-a (0.489), and phosphorus (0.390). This component represents a trophic gradient related to the increase in nutrients, organic matter, and phytoplankton biomass in the reservoirs. The second principal component (PC2) is primarily driven by nitrogen which exhibits a high positive load (0.797), indicating a secondary gradient related to this parameter. Phosphorus (0.468), turbidity (0.129), and chlorophyll a (0.039) have a lesser influence on this axis. Overall, the results suggest that PC1 captures the combined variability of key trophic indicators, whereas PC2 mainly reflects variations associated with nitrogen dynamics

Table 5. Factorial loads of the main water quality parameters in the first two principal components (PC1 and PC2), indicating the weight of each variable in the multivariate structure of the data.

Parameter	PC1	PC2
Phosphorus	0.390	0.467
Nitrogen	-0.128	0.797
Chlorophyll	0.488	0.037
COD	0.493	-0.357
Turbidity	0.592	0.131

The scatter plot shown in Figure 8 indicates that high Forel-Ule Index (FUI) values (brownish points) are predominantly located in the positive quadrant of PC1, indicating environments with higher turbidity and nutrient concentration. In contrast, samples with values below the FUI index, represented by the blue and green points, are in the negative quadrant of PC1, representing waters with greater transparency and reduced concentrations of nutrients, organic matter, and chlorophyll-a, resulting in a lower trophic state.

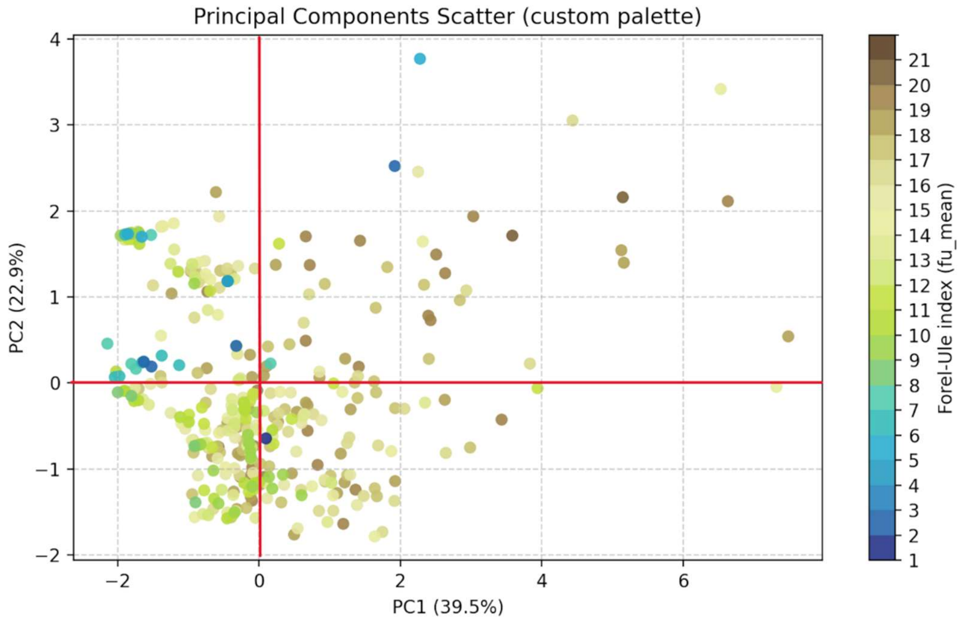

Figure 8. Distribution of sample data in the first two principal components (PC1 and PC2), highlighting the gradient of the Forel-Ule index (FU_mean) using a color scale. More yellowish points indicate higher FU_mean values, while bluish tones correspond to lower values.

The second component (PC2) was mainly characterized by the contribution of nitrogen, reflecting a secondary environmental gradient possibly related to the dynamics of this nutrient in water bodies. However, no statistically significant association with the Forel-Ule index was observed (Table 6). In contrast, the correlations between FUI_mean and PC1 were positive and statistically significant ($p < 0.001$), with coefficients Pearson and Spearman ranging from 0.375 and 0.439, respectively, indicating a low to moderate intensity association (Figure 9).

Table 6. Correlation coefficients (Pearson, Spearman) and respective p-values between the Forel-Ule index (FU_mean) and the principal components PC1 and PC2.

Method	Coef (PC1)	p-value (PC1)	Coef (PC2)	p-value (PC2)
Pearson	0.375	0.000	-0.091	0.07
Spearman	0.439	0.000	-0.058	0.247

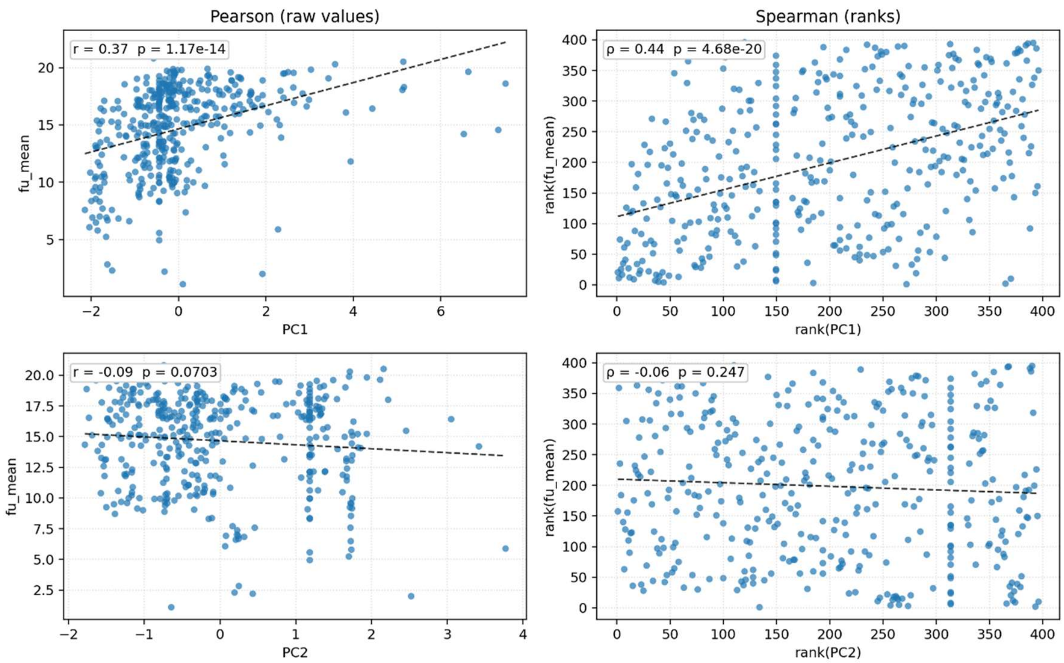

Figure 9. Correlations between the Forel–Ule Index (FUI) and the first two principal components: left, Pearson (raw values) for FUI×PC1 and FUI×PC2; right, Spearman (ranks) for the same pairs, with trend lines and statistics (r, ϱ, p). A positive, significant association is observed only with PC1, consistent with the trophic–optical gradient; PC2 shows no significant correlation. Note: vertical/horizontal alignments arise from ties introduced by median imputation (multiple cases sharing the same value).

4.3. FUI and Ecological Status

The results of the ordinal logistic regression, conducted to assess the capacity of the Forel-Ule Index (FUI) to predict the ecological status of reservoirs indicate that the model successfully captured the expected ordinal gradient between the quality classes “GOOD”, “MODERATE”, “POOR” and “BAD”. A consistent relationship was observed between the mean FUI value recorded for each reservoir and the corresponding ecological status classification (Table 7).

At low FUI values (between 10 and 13), the probability associated with the “GOOD” class was high, often exceeding 0.70, resulting in projected classifications consistent with the observed data, as in the Beliche and Minutos reservoirs (Cycle 2) and Odeleite (Cycles 2 and 3). This suggests that the model can identify the best ecological quality conditions associated with clearer waters

At intermediate FUI values (between 14 and 16), there was greater uncertainty in the projection, with a distribution of probabilities between the “GOOD,” “MODERATE,” and “POOR” classes. For example, in the Caia reservoir (Cycle 3, FUI = 14), the observed class was MODERATE, but the model projected the GOOD class with a probability of 0.57. In the Alvito reservoir (Cycle 2, FUI = 15), the observed class was “GOOD,” but the model projected a 54% probability of ‘MODERATE’ and a 41% probability of “GOOD.” In the Maranhão reservoir (Cycle 3, FUI = 16), the observed class was POOR, but the projected class was MODERATE with a 65% probability.

For FUI values greater than 16, the model systematically projects the class “Moderate”. The Campilhas, Monte da Rocha, and Pego do Altar reservoirs in the second cycle were all classified as

doi:10.20944/preprints202603.0477.v1

'GOOD' under the monitoring system, but the model projected them as "MODERATE," with a probability greater than 0.60 for this class. In the third cycle, cases such as Divor (classified as BAD) and Magos and Maranhão (classified as POOR) were projected as MODERATE, with probabilities close to 0.70.

Table 7. Results of the ordinal logistic regression for cycles 2 and 3, showing the mean Forel-Ule Index (FUI), observed and projected ecological status, and predicted probabilities for each class (Good, Moderate, Poor, Bad).

Cycle	Reservoir	FUI mean	Ecological status	Projected	Probability Good	Probability Moderate	Probability Poor	Probability Bad
Second	Alvito	15	Good	Moderate	0.41	0.54	0.03	0.01
	Beliche	10	Good	Good	0.95	0.05	0.00	0.00
	Caia	15	Moderate	Moderate	0.40	0.56	0.03	0.01
	Campilhas	17	Good	Moderate	0.17	0.69	0.09	0.04
	Divor	17	Moderate	Moderate	0.17	0.69	0.09	0.05
	Magos	17	Moderate	Moderate	0.19	0.69	0.08	0.04
	Maranhao	16	Moderate	Moderate	0.26	0.66	0.06	0.03
	Minutos	13	Good	Good	0.73	0.26	0.01	0.00
	Montargil	16	Moderate	Moderate	0.28	0.64	0.05	0.02
	Monte da Rocha	17	Good	Moderate	0.17	0.69	0.09	0.05
	Monte Novo	17	Moderate	Moderate	0.15	0.70	0.10	0.05
	Odeleite	10	Good	Good	0.94	0.06	0.00	0.00
	Odivelas	14	Good	Good	0.55	0.42	0.02	0.01
	Pego do Altar	17	Good	Moderate	0.15	0.70	0.10	0.05
	Roxo	15	Good	Moderate	0.38	0.57	0.03	0.02
	Vale do Gaio	17	Moderate	Moderate	0.18	0.69	0.09	0.04
	Vigia	16	Moderate	Moderate	0.32	0.62	0.04	0.02
Third	Alvito	14	Moderate	Good	0.67	0.32	0.01	0.00
	Beliche	14	Good	Good	0.66	0.32	0.01	0.00
	Caia	14	Moderate	Good	0.57	0.40	0.02	0.01
	Campilhas	18	Moderate	Moderate	0.13	0.69	0.12	0.06
	Divor	17	Bad	Moderate	0.17	0.69	0.09	0.05
	Magos	17	Poor	Moderate	0.16	0.70	0.10	0.05
	Maranhao	16	Poor	Moderate	0.27	0.65	0.05	0.03
	Minutos	16	Good	Moderate	0.34	0.60	0.04	0.02
	Montargil	16	Moderate	Moderate	0.24	0.67	0.06	0.03
	Monte da Rocha	18	Moderate	Moderate	0.10	0.68	0.14	0.08
	Monte Novo	18	Moderate	Moderate	0.12	0.69	0.12	0.07
	Odeleite	13	Good	Good	0.70	0.29	0.01	0.00
	Odivelas	14	Moderate	Good	0.56	0.42	0.02	0.01
	Pego do Altar	17	Moderate	Moderate	0.18	0.69	0.09	0.04
	Roxo	16	Moderate	Moderate	0.36	0.59	0.04	0.02
	Vale do Gaio	17	Moderate	Moderate	0.17	0.69	0.09	0.04
	Vigia	17	Moderate	Moderate	0.20	0.69	0.08	0.04

The assessment of the ecological status of water bodies is composed of different components: biological, physicochemical, hydromorphological, and specific pollutants. However, the application of ordinal logistic regression was focused only on the biological and physicochemical components, as these most closely correspond to the bio-optical influences that determine water color and, consequently, the FUI (Table 8). The biological component is represented by phytoplankton and chlorophyll-a, variables directly associated with the productivity and trophic state of the aquatic

Preprints.org (www.preprints.org) | NOT PEER-REVIEWED | Posted: 5 March 2026 doi:10.20944/preprints202603.0477.v1

system. The physicochemical component encompasses the concentration of phosphorus and nitrogen, nutrients that indirectly regulate phytoplankton biomass and, therefore, significantly influence the optical response captured by the FUI.

The respective explanatory variables and predictors derived from the dataset were used. This approach allowed us to assess the extent to which the predictors capture the variability observed in each component and adequately correspond to the classifications obtained in situ. The biological component assessment showed a heterogeneous distribution among the predicted quality classes, particularly in the "GOOD" and "MODERATE" categories. In reservoirs with low IUF values, such as Odeleite (IUF = 10–13), the observed biological component was classified as "Excellent" or "Good," and the predicted values tended to follow the same trend.

In reservoirs with intermediate FUI values (14–16), greater inconsistencies were found. In the Alvito and Odivelas reservoirs, for example, the observed biological component was classified as "Good," while the predicted component varied between "Good" and "Moderate," revealing that the model tends to confuse the classification in certain contexts. In contrast, in other reservoirs with similar FUI values, such as Roxo, there was greater convergence between the two approaches, with both results aligned in the "MODERATE" category. In the most turbid reservoirs, with FUI values ≥ 17, the observed biological classification was concentrated in the "MODERATE" category. In these cases, predictions generally followed observations, but with an occasional tendency to indicate a condition one level higher, as in Divor, Magos, and Maranhão in the third cycle, where the model estimated "Fair" compared to the worst observed conditions. This discrepancy suggests that predictors are less sensitive to capturing the negative extremes of the biological gradient.

The physicochemical component predominantly revealed observed classifications in the "GOOD" and "MODERATE" categories. The predicted values followed this trend. In reservoirs with lower FUI values (10–13), such as Beliche and Odeleite, there was agreement between the observed and predicted values, with both falling into the highest physicochemical quality classes (GOOD), confirming the expected relationship between lower FUI values and better environmental conditions. In contrast, in reservoirs with higher FUI values (≥ 17), both observed and predicted classifications tended to fall into the MODERATE category.

However, in intermediate situations (FUI between 14 and 16), discrepancies between the observed and predicted values were frequently observed. In some cases, such as Alvito and Caia, the model overestimated quality by classifying observed conditions as "MODERATE" as "GOOD." However, in other reservoirs with FUI values between 14 and 16, such as Beliche, Minutos, Montargil, and Roxo, in the third cycle, there were underestimates between the results, with both approaches converging to a predicted classification lower than the observed one (Table 8).

Table 8. Results of the ecological status assessment for the reservoirs, showing the mean Forel-Ule Index (FUI), observed biological and physico-chemical components, their respective predictors, and the overall classification in each quality class (Excellent, Good, Moderate, Poor, Bad).

	Reservoir	Forel-Ule mean	Biological component	Biological predictor	Physico-chemical component	Physico-chemical predictor
Second Cicle	Alvito	15	Good	Moderate	Moderate	Good
	Beliche	10	Good	Good	Excellent	Good
	Caia	15	Good	Moderate	Moderate	Good
	Campilhas	17	Moderate	Moderate	Good	Moderate
	Divor	17	Moderate	Moderate	Moderate	Moderate
	Magos	17	Moderate	Moderate	Moderate	Moderate
	Maranhao	16	Good	Good	Moderate	Moderate
	Minutos	13	Moderate	Moderate	Good	Moderate
	Montargil	16	Good	Moderate	Good	Moderate
	Monte da Rocha	17	Moderate	Moderate	Moderate	Moderate
	Monte Novo	17	Good	Good	Moderate	Moderate
	Odeleite	10	Good	Good	Excellent	Good
	Odivelas	14	Good	Moderate	Good	Good

	Pego do Altar	17	Good	Moderate	Moderate	Moderate
	Roxo	15	Moderate	Moderate	Good	Moderate
	Vale do Gaio	17	Moderate	Moderate	Moderate	Moderate
	Vigia	16			Moderate	Moderate
Third cicle	Alvito	14	Moderate	Good	Good	Good
	Beliche	14	Excellent	Good	Good	Good
	Caia	14	Good	Good	Moderate	Good
	Campilhas	18	Moderate	Moderate	Good	Moderate
	Divor	17	Bad	Moderate	Moderate	Moderate
	Magos	17	Poor	Moderate	Moderate	Moderate
	Maranhao	16	Poor	Moderate	Moderate	Moderate
	Minutos	16	Good	Moderate	Good	Good
	Montargil	16	Moderate	Moderate	Moderate	Moderate
	Monte da Rocha	18	Moderate	Moderate	Good	Moderate
	Monte Novo	18	Moderate	Moderate	Moderate	Moderate
	Odeleite	13	Excellent	Good	Good	Good
	Odivelas	14	Moderate	Good	Good	Good
	Pego do Altar	17	Moderate	Moderate	Good	Moderate
	Roxo	16	Moderate	Moderate	Good	Good
	Vale do Gaio	17	Moderate	Moderate	Moderate	Moderate
	Vigia	17	Moderate	Moderate	Moderate	Moderate

5. Discussion

5.1. Seasonality of FUI in the Study Area

The high variability of FUI across reservoirs reflects pronounced environmental heterogeneity that cannot be explained solely by their physical characteristics, such as reservoir size. Reservoir conditions are influenced by multiple interacting factors, particularly surrounding land cover and nutrient inputs associated with anthropogenic pressures (Ma et al., 2023). Forested areas tend to reduce the surface runoff of pollutants, whereas urbanised and agricultural areas constitute major sources of diffuse pollution. Consequently, landscape connectivity with the water body emerges as a key mechanism controlling the optical properties of the water and, ultimately, the distinct FUI patterns observed among reservoirs.

Nutrient inputs are closely associated with precipitation, as higher FUI values tend to follow episodes of increased rainfall. Enhanced surface runoff during these periods promotes the transport of nutrients and organic matter into reservoirs, potentially intensifying soil erosion and contributing to surface water contamination through the mobilisation of sediments, fertilisers, and other agrochemicals applied to cultivated land. Figure 10 suggests a potential relationship between rainfall episodes and increased FUI variability over the analysed period. Months with the highest precipitation peaks (December and January) exhibit a slight increase in FUI values, whereas months with the lowest precipitation (June, July, and August) correspond to the lowest index values.

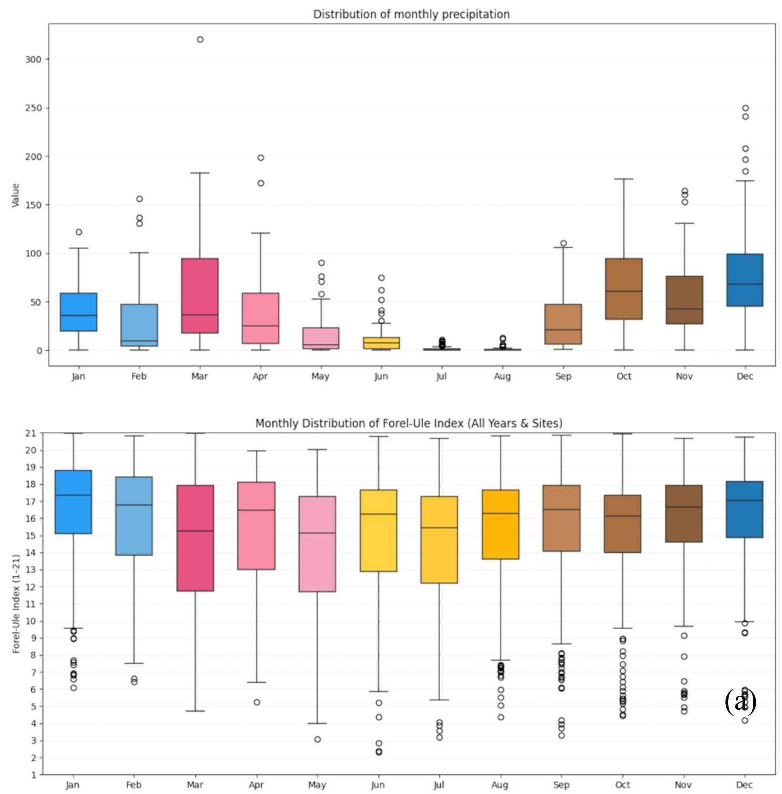

Figure 10. (a) Monthly distribution of precipitation from October 2017 to September 2024, based on data from 16 meteorological stations located near the study reservoirs. (b) Monthly distribution of mean Forel–Ule Index (FUI) values from October 2017 to September 2024.

Several studies associate increased precipitation with higher FUI values. For example, Li et al. (2024) demonstrated that continuous rainfall driven by a quasi-stationary front in southern China during late spring directly influenced FUI dynamics in urban lakes, including the Zhinyin Reservoir. The increase in FUI closely followed the average monthly precipitation pattern, with rainfall peaking in June (10,444.4 mm). This substantial volume of precipitation enhanced the transport of sediments and suspended particles into the lakes, leading to a marked increase in FUI values. Similarly, a study on large reservoirs in China (Lai et al., 2024) reported that, during the rainy season, most reservoir waters exhibited green to yellowish-green hues, accompanied by relatively higher FUI values compared to other seasons.

5.2. Relationship Between FUI and Water Quality Parameters

The first two principal components capture 62.4% of the total variance in the five variables, a result which is consistent with the PCA-based water quality literature. For example, Ibrahim et al. (2023), used 22 water quality parameters to investigate latent sources of pollution in rivers using PCA and generated six significant components that explained 65.4% of the variance in the water quality data.

The first component (PC1) explained 39% of the variance and showed positive loads for turbidity (0.59), COD (0.49), and chlorophyll-a (0.49). Considering the reference ranges for factor loadings suggested by Liu et al. (2003), turbidity indicates a moderate contribution (0.50–0.75), while COD and chlorophyll-a are at the upper limit of the weak range (0.30–0.50). As all loads are positive, the variables increase in the same direction as the component, characterizing a trophic gradient that integrates the joint variability associated with nutrient enrichment and phytoplankton biomass (Table 5).

 doi:10.20944/preprints202603.0477.v1

The concentration of samples with high FUI values in the positive quadrant of this axis (Figure 18) reinforces the interpretation that the optical index is related to more turbid and eutrophic environments The positive and significant correlations between PC1 and FUI (ϱ=0.439, p=4.68e-20), although of low to moderate magnitude, suggest that the index partially captures the trophic gradient synthesized by the first component.

Lai et al. (2024) applied PCA to eight water quality parameters (including total phosphorus, total nitrogen, and turbidity) and initially observed a weak correlation between FUI (derived from Landsat-8 OLI images) and the principal components. However, subsequent analyses showed that the relationship between FUI and turbidity is dependent on the index level itself: the correlation was low for FUI < 12 (R = 0.37), becoming high for FUI > 12 (R = 0.80). These results indicate that, in more turbid waters (FUI > 12), turbidity becomes the predominant factor controlling water color. Finally, the authors demonstrated that FUI > 15 is a clear discriminator of turbid waters, corresponding to more than 85% of the water body area classified as turbid.

The second component (PC2), which explains 23% of the variance and is characterized mainly by nitrogen, expresses a secondary environmental gradient, possibly associated with the specific dynamics of this nutrient. However, the absence of a statistically significant correlation between PC2 and FUI (ϱ= -0.06, p=0.247) indicates that the variability explained by this axis does not translate into noticeable differences in water color.

The multivariate analysis indicates that the Forel–Ule Index (FUI) can be interpreted as an indirect indicator of water trophic status, primarily driven by turbidity, while showing limited sensitivity to processes governed by isolated variables such as nitrogen. These findings reinforce the potential of the FUI as a metric of the optical and trophic conditions of reservoirs, while also highlighting the need to complement it with detailed physicochemical measurements to achieve a more robust ecological assessment.

5.3. FUI and the Water Framework Directive

Considering the limitations imposed by the evaluation cycles of Directive 2000/60/EC, with long intervals and temporal gaps in the *in situ* data, the FUI emerges as a complementary metric capable of offering greater temporal resolution and reduced cost. From this perspective, ordinal logistic regression translates FUI values into probabilities of classification into ecological classes, associating an optical indicator with the regulatory parameter.

Ordinal logistic regression confirmed the ability of the FUI to reflect the ordinal gradient of ecological quality, with good performance especially at low values (10-14), where the probability of classification as Good was greater than 0.70. This result reinforces the potential of the FUI to capture conditions associated with better ecological status. However, in the intermediate and high FUI ranges (>15), the model showed greater uncertainty, with the Good, Moderate, and Poor classes being predominantly projected as Moderate. These classes represent gradual ecological transitions, in which small variations in water coloration can result in category changes. This overlap can be explained by the borderline nature of the classes, which are simultaneously influenced by different assessment components (biological, physical-chemical, hydromorphological, and pollutants).

The statistical analysis was conditioned by the existing dataset. In the official WFD dataset, the *Poor* category, for example, appears only for the Magos and Maranhão reservoirs in the Third Cycle, which limits the statistical performance of logistic regression and redistributes the probability of high FUI values to adjacent and more representative classes, such as *Moderate*. Thus, the behavior of the model reproduces the gradual logic of the WFD assessment process, highlighting the importance of a cautious interpretation of FUI values in situations of category transition

When evaluating the capacity of the FUI to predict overall ecological status, it is important to consider that, under the WFD, classification follows the "one-out, all-out" principle, whereby the overall status of a water body is determined by the lowest category assigned to any of the assessed quality elements (European Union, 2000). Consequently, even if most indicators are classified as

 doi:10.20944/preprints202603.0477.v1

"Good," a single result rated as "Moderate" automatically lowers the overall ecological status to that level.

To further explore this issue, the physico-chemical and biological components were modelled separately, yielding comparable results. In reservoirs with FUI values between 10 and 14, a high level of agreement between observed and predicted classifications was obtained for both components. Of the nine in situ observations within this FUI range, six were predicted as "Good" for the biological component and seven for the physico-chemical component. For moderate to high FUI values (>15), both components were predominantly classified as "Moderate," reflecting the same uncertainties observed in the prediction of overall ecological status.

These results support the use of the Forel-Ule Index as a complementary tool to conventional monitoring, particularly effective in identifying good ecological conditions and cleaner waters. However, its application requires cautious interpretation for FUI values above 15, where gradual transitions in ecological status associated with increased turbidity and water coloration predominate. In these contexts, the FUI can act as a sensitive indicator of progressive changes toward ecological deterioration, providing a faster response and support for environmental management.

6. Conclusions

In this study, turbidity was the parameter most significantly associated with FUI in the reservoirs analysed. PC1 acts as a trophic gradient, which is clearly reflected by FUI, reinforcing the conclusion that this index is an effective proxy for indicating eutrophication and turbidity conditions in reservoirs.

The trophic dynamics in question are associated with the seasonality of precipitation. As demonstrated in the literature, rainfall peaks (autumn/winter) generate surface runoff that intensifies the input of sediments, nutrients, and organic matter. This external input mechanism is the interfering factor that increases water turbidity, creating the high load conditions observed in the positive quadrant of PC1 and, consequently, in the higher FUI values.

This is also consistent with the result of the ordinal logistic regression, in which the WQA classes (in situ data) are the response and the FUI is the predictor. The good performance of FUI values below 13 in detecting the 'Good' class corroborates its effectiveness as a screening indicator for clean and stable water bodies. However, the uncertainty of the model in the intermediate ranges shows that, from FUI values above 14 and, more critically, its tendency to underestimate 'Poor' or 'Bad' states at high FUI values (>15), reflects a limitation. According to the 'one out, all out' rule of the WFD, even slight variations in FUI/turbidity can result in a downgrading of the overall classification for border zones. High turbidity induced by precipitation, when the optical medium is saturated, is evidenced by the FUI, which indicates an increase in turbidity but has a lower capacity to discriminate the nuances of chemical degradation.

In view of the above, it can be inferred that FUI is a complementary predictive indicator for screening and early warning when there is an increase in precipitation, with high utility for identifying waters in good condition and signaling transitions, since the WFD establishes as a central goal the maintenance or achievement of 'good ecological status'. For greater accuracy, it should be complemented by physical-chemical and biological metrics when fine discrimination between classes is decisive, to support official assessment and optimize the allocation of efforts in *in situ* monitoring campaigns.

Author Contributions: Conceptualization, Mariana Campista Chagas, Ana Paula Falcão and Rodrigo Proença de Oliveira; Methodology, Mariana Campista Chagas, Ana Paula Falcão and Rodrigo Proença de Oliveira; Software, Mariana Campista Chagas; Validation, Ana Paula Falcão and Rodrigo Proença de Oliveira; Formal analysis, Mariana Campista Chagas; Writing – original draft, Mariana Campista Chagas; Writing – review & editing, Ana Paula Falcão and Rodrigo Proença de Oliveira; Supervision, Ana Paula Falcão and Rodrigo Proença de Oliveira. All authors have read and agreed to the published version of the manuscript.

Funding: This research was funded by Fundação para a Ciência e Tecnologia, grant number UI/BD/151426/2021.

 doi:10.20944/preprints202603.0477.v1

Data Availability Statement: The Sentinel-2 datasets are publicly available through the Copernicus Open Access Hub (https://scihub.copernicus.eu/). Hydrological and reservoir monitoring data were obtained from the Portuguese National Water Resources Information System (SNIRH, https://snirh.apambiente.pt/) and the Portuguese Environment Agency (APA). Additional data and scripts used for the analysis are available from the corresponding author upon reasonable request.

Acknowledgments: The authors would like to thank the Portuguese Environment Agency (APA) for providing infrastructure and monitoring data, and the Foundation for Science and Technology (FCT) for the doctoral grant UI/BD/151426/2021. This work is part of the research activities developed at the Research and Innovation Center in Civil Engineering for Sustainability (CERIS) and was funded by the Foundation for Science and Technology (FCT).

Conflicts of Interest: The authors affirm that there are no known conflicts of interest or personal affiliations that may have affected the objectivity or integrity of the work presented in this article.

References

1. **Agência Portuguesa do Ambiente (APA).** (2022). *Guadiana River Management Plan (2022–2027).* Amadora, Portugal: Agência Portuguesa do Ambiente.
2. **Agência Portuguesa do Ambiente (APA).** (2023). *Sado and Mira River Management Plan (2022–2027).* Amadora, Portugal: Agência Portuguesa do Ambiente.
3. **Almeida, C., Ramos, T., Segurado, P., Branco, P., Neves, R., & Oliveira, R.** (2018). Water quantity and quality under future climate and societal scenarios: A basin-wide approach applied to the Sorraia River, Portugal. *Water, 10*(9), 1186. https://doi.org/10.3390/w10091186
4. **Alqueva Development and Infrastructure Company (EDIA).** (2024). *Institutional website.* Retrieved March 10, 2024, from https://www.edia.pt
5. **Batista, M., Abreu, M., Locutura, J., Oliveira, D., Matos, J., Silva, C., ... & Martins, L.** (2012). Evaluation of trace elements mobility from soils to sediments between the Iberian Pyrite Belt and the Atlantic Ocean. *Journal of Geochemical Exploration, 123,* 61–68. https://doi.org/10.1016/j.gexplo.2012.06.011
6. **Chen, X., Liu, L., Zhang, X., Li, J., Wang, S., Liu, D., Duan, H., & Song, K.** (2021). An assessment of water color for inland water in China using a Landsat 8-derived Forel-Ule index and the Google Earth Engine platform. *IEEE Journal of Selected Topics in Applied Earth Observations and Remote Sensing, 14,* 5773–5784. https://doi.org/10.1109/JSTARS.2021.3085411
7. **European Environment Agency.** (1996). *Water resources problems in southern Europe: An overview report* (Topic Report No. 15/1996). Copenhagen, Denmark: European Environment Agency.
8. **European Union.** (2000). Directive 2000/60/EC of the European Parliament and of the Council of 23 October 2000 establishing a framework for Community action in the field of water policy. *Official Journal of the European Communities, L 327,* 1–73.
9. **Gardner, J. R., Yang, X., Topp, S. N., Ross, M. R. V., Altenau, E. H., & Pavelsky, T. M.** (2021). The color of rivers. *Geophysical Research Letters, 48*(1), e2020GL088946. https://doi.org/10.1029/2020GL088946
10. **Garel, E., & Ferreira, Ó.** (2015). Multi-year high-frequency physical and environmental observations at the Guadiana Estuary. *Earth System Science Data, 7*(2), 299–309. https://doi.org/10.5194/essd-7-299-2015
11. **Greenhouse, J. B., Bromberg, J. A., & Fromm, D.** (1995). An introduction to logistic regression with an application to the analysis of language recovery following a stroke. *Journal of Communication Disorders, 28*(3), 229–246. https://doi.org/10.1016/0021-9924(94)00011-N
12. **Hotelling, H.** (1933). Analysis of a complex of statistical variables into principal components. *Journal of Educational Psychology, 24,* 417–520.
13. **Ibrahim, A., Ismail, A., Juahir, H., Iliyasu, A. B., Wailare, B. T., Mukhtar, M., & Aminu, H.** (2023). Water quality modelling using principal component analysis and artificial neural network. *Marine Pollution Bulletin, 187,* 114493. https://doi.org/10.1016/j.marpolbul.2022.114493
14. **Lai, Y., Zhang, J., Li, W., & Song, Y.** (2024). Water quality monitoring of large reservoirs in China based on water color change from 1999 to 2021. *Journal of Hydrology, 633,* 130988. https://doi.org/10.1016/j.jhydrol.2024.130988

 doi:10.20944/preprints202603.0477.v1

15. **Lehmann, M. K., Nguyen, U., Allan, M., & Van der Woerd, H. J.** (2018). Color classification of 1,486 lakes over a wide range of optical water types. *Remote Sensing*, *10*(8), 1273.
16. **Li, L., Ning, Y., Cao, Z., Xue, K., & Song, C.** (2024). A national-scale assessment on the spatial and temporal variations in water color for urban lakes in China. *Science of the Total Environment*, *945*, 173951. https://doi.org/10.1016/j.scitotenv.2024.173951
17. **Liu, C.-W., Lin, K.-H., & Kuo, Y.-M.** (2003). Aplicação da análise fatorial na avaliação da qualidade da água subterrânea em uma área afetada pela doença do pé preto em Taiwan. *Science of the Total Environment*, *313*(1–3), 77–89. https://doi.org/10.1016/S0048-9697(02)00683-6
18. **Ma, B., Wu, C., Jia, X., Zhang, Y., & Zhou, Z.** (2023). Predicting water quality using partial least squares regression of land use and morphology (Danjiangkou Reservoir, China). *Journal of Hydrology*, *624*, 129828. https://doi.org/10.1016/j.jhydrol.2023.129828
19. **Matono, P., Sousa, D., & Ilhéu, M.** (2013). Effects of land use intensification on fish assemblages in Mediterranean climate streams. *Environmental Management*, *52*(5), 1213–1229. https://doi.org/10.1007/s00267-013-0152-3
20. **McCullagh, P.** (1980). Regression models for ordinal data. *Journal of the Royal Statistical Society: Series B (Methodological)*, *42*(2), 109–142. https://doi.org/10.1111/j.2517-6161.1980.tb01109.x
21. **Molina-Navarro, E., Segurado, P., Branco, P., Almeida, C., & Andersen, H.** (2020). Predicting the ecological status of rivers and streams under different climatic and socioeconomic scenarios using Bayesian belief networks. *Limnologica*, *80*, 125742. https://doi.org/10.1016/j.limno.2019.125742
22. **Mustapha, A., Aris, A. Z., Ramli, M. F., & Juahir, H.** (2012). Aspectos temporais da variação da qualidade da água superficial utilizando ferramentas estatísticas robustas. *The Scientific World Journal*, *2012*, 294540. https://doi.org/10.1100/2012/294540
23. **Nascimento, Â., Biguino, B., Borges, C., Cereja, R., Cruz, J., Sousa, F., ... & Brito, A.** (2021). Tidal variability of water quality parameters in a mesotidal estuary (Sado estuary, Portugal). *Scientific Reports*, *11*(1). https://doi.org/10.1038/s41598-021-02603-6
24. **Palma, P., Alvarenga, P., Palma, V., Fernandes, R., Soares, A., & Barbosa, I.** (2009). Assessment of anthropogenic sources of water pollution using multivariate statistical techniques: A case study of the Alqueva's reservoir, Portugal. *Environmental Monitoring and Assessment*, *165*(1–4), 539–552. https://doi.org/10.1007/s10661-009-0965-y
25. **Rocha, M., & Rocha, E.** (2023). Chemical survey and risk assessment of 56 pesticides in the Sado River estuary (Iberian Peninsula, Portugal). *Toxics*, *11*(5), 457. https://doi.org/10.3390/toxics11050457
26. **Rocha, M., Cruzeiro, C., Reis, M., Rocha, E., & Pardal, M.** (2013). Determination of 17 endocrine disruptor compounds and their spatial and seasonal distribution in the Sado River estuary (Portugal). *Toxicological and Environmental Chemistry*, *95*(2), 237–253. https://doi.org/10.1080/02772248.2012.758730
27. **Sampath, D., & Boski, T.** (2016). Morphological response of the saltmarsh habitats of the Guadiana estuary due to flow regulation and sea-level rise. *Estuarine, Coastal and Shelf Science*, *183*, 314–326. https://doi.org/10.1016/j.ecss.2016.07.009
28. **Santos, L. P. dos, & Silva, M. G. da.** (2018). Water management and monitoring: An approach to legislation in Portugal and Brazil. *Ibero-American Journal of Humanities, Sciences and Education*, *4*(2), 37–54. https://doi.org/10.51891/revistahum.v4i2.295
29. **Sent, G., Biguino, B., Favareto, L., Cruz, J., Sá, C., Dogliotti, A., ... & Brito, A.** (2021). Deriving water quality parameters using Sentinel-2 imagery: A case study in the Sado estuary, Portugal. *Remote Sensing*, *13*(5), 1043. https://doi.org/10.3390/rs13051043
30. **Song, T., Liu, G., Zhang, H., Yan, F., Fu, Y., & Zhang, J.** (2023). Lake cyanobacterial bloom color recognition and spatiotemporal monitoring with Google Earth Engine and the Forel-Ule Index. *Remote Sensing*, *15*, 3541. https://doi.org/10.3390/rs15143541
31. **Wang, S., Li, J., Shen, Q., Zhang, B., Zhang, F., & Lu, Z.** (2015). MODIS-based radiometric color extraction and classification of inland water with the Forel-Ule scale: A case study of Lake Taihu. *IEEE Journal of Selected Topics in Applied Earth Observations and Remote Sensing*, *8*(2), 907–918. https://doi.org/10.1109/JSTARS.2014.2360564

 doi:10.20944/preprints202603.0477.v1

32. **Xia, K., Wu, T., Li, X., Wang, S., & Shen, Q.** (2024). A new method for accurate inversion of Forel-Ule index using MODIS images – Revealing the water color evolution in China's large lakes and reservoirs over the past two decades. *Water Research, 255,* 121560. https://doi.org/10.1016/j.watres.2024.121560
33. **Ye, M., & Sun, Y.** (2022). Review of the Forel-Ule Index based on in situ and remote sensing methods and application in water quality assessment. *Environmental Science and Pollution Research, 29*(9), 13024–13041. https://doi.org/10.1007/s11356-021-18083-0
34. **Ying, H., Wang, S., Zhang, B., Mao, Z., Zhang, F., & Li, J.** (2024). Earth observation reveals the shifting patterns of China's lake color driven by climate change and land cover. *Journal of Environmental Management, 370,* 122809. https://doi.org/10.1016/j.jenvman.2024.122809
35. **Zhao, Y., Chen, J., & Li, X.** (2023). Sentinel-2 observation of water color variations in inland water across Guangzhou and Shenzhen after the establishment of the Guangdong–Hong Kong–Macao Bay Area. *Applied Sciences, 13,* 9039. https://doi.org/10.3390/app13159039
36. **Zhou, Y., He, B., Fu, C., Giardino, C., Bresciani, M., Liu, H., Feng, Q., Xiao, F., Zhou, X., & Liang, S.** (2021). Assessments of trophic state in lakes and reservoirs of Wuhan using Sentinel-2 satellite data. *European Journal of Remote Sensing, 54*(1), 461–475. https://doi.org/10.1080/22797254.2021.1960201
37. **Zhou, Y., He, B., Fu, C., Xiao, F., Feng, Q., Liu, H., Zhou, X., Yang, X., & Du, Y.** (2021). An improved Forel-Ule index method for trophic state assessments of inland waters using Landsat 8 and Sentinel archives. *GIScience & Remote Sensing, 58*(8), 1316–1334. https://doi.org/10.1080/15481603.2021.1987003
38. **Jolliffe, I. T., & Cadima, J. (2016).** Principal component analysis: a review and recent developments. Philosophical Transactions of the Royal Society A, 374(2065), 20150202. https://doi.org/10.1098/rsta.2015.0202
39. Hair, J. F., Black, W. C., Babin, B. J., & Anderson, R. E. (2019). Multivariate Data Analysis (8th ed.). Cengage.